Inorg. Chem. **1989**, *28*, 2107–2113

Contribution from the School of Chemical Sciences,
The University of Illinois at Urbana-Champaign, Urbana, Illinois 61801

Synthesis, Characterization, and X-ray Crystal Structures of the Divalent Titanium Complex $Ti(\eta^2-BH_4)_2(dmpe)_2$ and the Unidentate Tetrahydroborate Complex $V(\eta^1-BH_4)_2(dmpe)_2$

James A. Jensen[†] and Gregory S. Girolami*

Received August 3, 1988

The reaction of the coordination complexes $MCl_2(dmpe)_2$, dmpe = 1,2-bis(dimethylphosphino)ethane, with $LiBH_4$ or $NaBH_4$ leads to the divalent transition-metal tetrahydroborate complexes $M(BH_4)_2(dmpe)_2$, where M is Ti or V. The titanium complex is a thermally robust and oxidatively stable paramagnetic species with very weakly bound bidentate BH_4^- groups based on infrared spectroscopy. The X-ray crystal structure of $Ti(\eta^2-BH_4)_2(dmpe)_2$ reveals that this compound adopts an eight-coordinate geometry related to a square-prismatic structure that is, however, best described as a trans octahedron with the bidentate BH_4^- groups occupying the axial sites. The two independent Ti–P distances are 2.627 (1) and 2.625 (1) Å, while the bidentate tetrahydroborate groups are bonded to the titanium center with distances of $Ti-H_b$ = 2.04 (2) and 2.09 (2) Å and Ti···B = 2.534 (3) Å. The H–B–H angles are all near the tetrahedral value of 109°, which is consistent with the weak $Ti-BH_4$ interaction deduced by IR spectroscopy. A correlation of the average $B-H_t$ and $B-H_b$ IR stretching frequencies for a variety of bidentate tetrahydroborate complexes in the literature provides a useful gauge of the relative strengths of $M-BH_4$ interactions. Crystal data for $C_{12}H_{40}B_2P_4Ti$: space group $P2_1/n$, $a = 9.404$ (2) Å, $b = 13.088$ (2) Å, $c = 9.466$ (2) Å, $\beta = 96.12$ (1)°, $V = 1158.4$ (4) Å^3, $Z = 2$, $R_F = 3.6\%$, $R_{wF} = 3.5\%$ for 2139 reflections and 168 variables. In contrast to the titanium results, the IR spectrum of the vanadium complex is indicative of unidentate BH_4^- coordination, as shown by the strong BH_3 deformation mode at 1057 cm^{-1}. The X-ray crystal structure of $V(\eta^1-BH_4)_2(dmpe)_2$ confirms this assignment; this is the first molecule that possesses more than one unidentate BH_4^- group and is of additional interest since, unlike most other η^1-BH_4 complexes, its electron count is less than 18. The vanadium center adopts a trans octahedral structure, with V–P = 2.499 (1) and 2.506 (1) Å, V–H = 1.88 (3) Å, V···B = 2.833 (4) Å, and V–H–B = 140 (3)°. Crystal data for $C_{12}H_{40}B_2P_4V$: space group $P2_1/n$, $a = 8.469$ (2) Å, $b = 13.735$ (4) Å, $c = 9.666$ (7) Å, $\beta = 96.14$ (3)°, $V = 1118$ (2) Å^3, $Z = 2$, $R_F = 3.2\%$, $R_{wF} = 3.0\%$ for 1629 reflections and 168 variables. The differences in the structures of $Ti(BH_4)_2(dmpe)_2$ and $V(BH_4)_2(dmpe)_2$ may be ascribed to the smaller atomic radius of vanadium and to the preference of d^3 V^{II} centers to adopt six-coordinate geometries. Attempts to prepare the analogous chromium(II) complex lead instead to the paramagnetic hydride complex $Cr(\eta^1-BH_4)H(dmpe)_2$, which possesses one unidentate BH_4^- ligand based on its IR spectrum. In the presence of $BH_3 \cdot L$, this complex is in equilibrium with $Cr(BH_4)_2(dmpe)_2$ in solution. A comparative summary is presented of the structural parameters of unidentate BH_4^- complexes of the transition metals, and a reaction coordinate is mapped out for terminal–bridge hydrogen exchange processes involving tetrahydroborate groups.

Introduction

In recent years, transition-metal tetrahydroborate derivatives of early transition metals have received renewed interest due to their utility as precursors for solid-state borides,[1-5] transition-metal polyhydrides,[6-9] metal alkyls,[10] and olefin polymerization catalysts.[11] Of the three covalent binding modes displayed by BH_4^- groups, tridentate, bidentate, and unidentate, the latter was the most recently confirmed experimentally and remains the least well understood. Few examples of unidentate BH_4^- complexes are known: of these, only $Cu(\eta^1-BH_4)(PMePh_2)_3$,[12-14] $Cu(\eta^1-BH_4)[(PPh_2CH_2)_3CMe]$,[15,16] $FeH(\eta^1-BH_4)(dmpe)_2$,[17,18] and $Hf_2[N(SiMe_2CH_2PMe_2)_2]_2H_3(BH_4)_3$,[9] have been characterized structurally, while other examples have been formulated on spectroscopic grounds.[8,19-22] All of these complexes contain at most one unidentate BH_4^- group, and all but one are 18-electron species. Generally, the number of bridging hydrogens through which BH_4^- groups are bound to a metal center correlates with the number of vacant metal orbitals of suitable energy and symmetry.[23,24]

We now describe the synthesis and characterization of new divalent tetrahydroborate derivatives of titanium, vanadium, and chromium from the dichloro complexes $MCl_2(dmpe)_2$, dmpe = $Me_2PCH_2CH_2PMe_2$.[25] There are several aspects of particular interest in this system: (1) The titanium compound $Ti(BH_4)_2(dmpe)_2$ is eight-coordinate with bidentate BH_4^- groups, but there is an unusually weak $M-BH_4$ interaction in this molecule. We present a correlation of the $\nu(BH_b)$ and $\nu(BH_t)$ IR stretching frequencies that gauges the relative strengths of $M(\eta^2-BH_4)$ interactions. (2) The vanadium compound $V(BH_4)_2(dmpe)_2$, by contrast, is six-coordinate with *two unidentate* BH_4^- groups. The presence of η^1-BH_4 groups despite a low electron count of 15 is attributable to steric effects and the electronic preference of d^3 metal centers to adopt octahedral coordination environments. (3) The chromium complex $Cr(BH_4)H(dmpe)_2$ is a rare example of a paramagnetic hydride; this compound also possesses a unidentate BH_4^- group. Interestingly, addition of $BH_3 \cdot L$ converts this species

---

[†] Present address: Hercules Inc., Research Center, Wilmington, DE 19894.

(1) Jensen, J. A.; Gozum, J. E.; Pollina, D. M.; Girolami, G. S. *J. Am. Chem. Soc.* **1988**, *110*, 1643–1644.
(2) Wayda, A. L.; Schneemeyer, L. F.; Opila, R. L. *Appl. Phys. Lett.* **1988**, *53*, 361–363.
(3) Rice, G. W.; Woodin, R. L. *J. Am. Ceram. Soc.* **1988**, *71*, C181–C183.
(4) Gallagher, M. J.; Rhine, W. E.; Bowen, H. K. *Proceedings of the 3rd International Conference on Ultrastructure Processing of Ceramics, Glasses, and Composites*; Mackenzie, J. D., Ulrich, D. R., Eds.; Wiley: New York, 1987.
(5) Bonetti, R.; Comte, D.; Hinterman, H. E. *Proceedings of the 5th International Conference on Chemical Vapor Deposition*; Electrochemical Society: Princeton, NJ, 1975; p 495.
(6) James, B. D.; Nanda, R. K.; Wallbridge, M. G. H. *Inorg. Chem.* **1967**, *6*, 1979–1983.
(7) Otto, E. E. H.; Brintzinger, H. H. *J. Organomet. Chem.* **1978**, *148*, 29–33.
(8) Luetkens, M. L.; Huffman, J. C.; Sattelberger, A. P. *J. Am. Chem. Soc.* **1985**, *107*, 3361–3362.
(9) Fryzuk, M. D.; Rettig, S. J.; Westerhaus, A.; Williams, H. D. *Inorg. Chem.* **1985**, *24*, 4316–4325.
(10) Jensen, J. A.; Wilson, S. R.; Schultz, A. J.; Girolami, G. S. *J. Am. Chem. Soc.* **1987**, *109*, 8094–8095.
(11) Raum, A. L. J.; Fraser, D. A. British Patent 801401, 1958.
(12) Bommer, J. C.; Morse, K. W. *Inorg. Chem.* **1980**, *19*, 587–593.
(13) Kutal, C.; Grutsch, P.; Atwood, J. L.; Rogers, R. D. *Inorg. Chem.* **1978**, *17*, 3558–3562.
(14) Tagusagawa, F.; Fumagalli, A.; Koetzle, T. F.; Shore, S. G.; Schmitkons, T.; Fratini, A. V.; Morse, K. W.; Wei, C.-Y.; Bau, R. *J. Am. Chem. Soc.* **1981**, *103*, 5165–5171.
(15) Dapporto, P.; Midollini, S.; Orlandini, A.; Sacconi, L. *Inorg. Chem.* **1976**, *15*, 2768–2774.
(16) Ghilardi, C. A.; Midollini, S.; Orlandini, A. *Inorg. Chem.* **1982**, *21*, 4096–4098.
(17) Baker, M. V.; Field, L. D. *J. Chem. Soc., Chem. Commun.* **1984**, 996–997.
(18) Bau, R.; Yuan, H. S.; Baker, M. V.; Field, L. V. *Inorg. Chim. Acta* **1986**, *114*, L27–L28.
(19) Holah, D. G.; Hughes, A. N.; Wright, K. *Can. J. Chem.* **1974**, *52*, 2990–2999.
(20) Holah, D. G.; Hughes, A. N.; Hui, B. C. *Can. J. Chem.* **1976**, *54*, 320–328.
(21) Bommer, J. C.; Morse, K. W. *Inorg. Chem.* **1979**, *18*, 531–538.
(22) Barron, A. R.; Salt, J. E.; Wilkinson, G.; Motevalli, M.; Hursthouse, M. B. *Polyhedron* **1986**, *5*, 1833–1837.

0020-1669/89/1328-2107$01.50/0

to the bis(tetrahydroborate) complex $Cr(BH_4)_2(dmpe)_2$ in solution. (4) Structural comparisons of known unidentate tetrahydroborates reveal one possible reaction coordinate and transition-state geometry for terminal-bridge hydrogen exchange in transition-metal BH_4^- complexes. The reaction pathway indicated involves rotation of a BH_3 unit about a $B-H_b$ single bond, in agreement with earlier suggestions.

Results and Discussion

Synthesis and Characterization of $M(BH_4)_2(dmpe)_2$ Complexes. Interaction of $TiCl_2(dmpe)_2$, dmpe = 1,2-bis(dimethylphosphino)ethane, with excess $LiBH_4$ in diethyl ether followed by crystallization from toluene gives the divalent tetrahydroborate complex $Ti(\eta^2\text{-}BH_4)_2(dmpe)_2$ (**1**) in good yield.[10] The dark red prisms are surprisingly robust for a titanium(II) compound

$$TiCl_2(dmpe)_2 + 2LiBH_4 \rightarrow Ti(\eta^2\text{-}BH_4)_2(dmpe)_2 + 2LiCl$$

and oxidize only slowly in air over a period of hours. The magnetic moment of this d^2 complex is 2.6 μ_B, corresponding to a high-spin configuration with two unpaired electrons as is observed for the chloro precursor $TiCl_2(dmpe)_2$.[25] In this context it is interesting to note that the corresponding methyl derivative $TiMe_2(dmpe)_2$ is diamagnetic.[10]

The infrared spectrum of **1** shows two strong terminal boron–hydrogen stretching bands at 2336 and 2299 cm^{-1} and two strong bridging boron–hydrogen stretching bands at 2215 and 2170 cm^{-1} that are clearly indicative of a bidentate coordination mode for the BH_4^- ligands.[23] The corresponding deuterium-substituted complex $Ti(BD_4)_2(dmpe)_2$ exhibits strong B–D stretching modes at 1750, 1705, and 1662 cm^{-1}. The room-temperature ^1H NMR spectrum shows paramagnetically shifted and broadened resonances for the dmpe ligands but no signals for the tetrahydroborate groups, apparently due to the proximity of the BH_4^- ligands to the paramagnetic center.

The robust nature of **1** is manifested in the lack of chemical reactivity with substrates such as CO (4 atm), H_2 (5 atm), excess dmpe, NEt_3, C_2H_4, C_5Me_5H, PhCCH, and PhCCPh; in all of these cases **1** may be recovered in good yield from the reaction solutions. Attempts to sublime $Ti(\eta^2\text{-}BH_4)_2(dmpe)_2$ in vacuum yield instead the phosphine–borane adduct $dmpe{\cdot}BH_3$[26] and an intractable titanium-containing solid.

Few titanium tetrahydroborates have been described previously, and unlike **1**, all are trivalent. Among these are the cyclopentadienyl derivatives $Cp_2Ti(BH_4)$[27,28] and $[CpTi(BH_4)Cl]_2$,[29,30] the unstable binary tetrahydroborate $Ti(BH_4)_3$,[31] and various Lewis base adducts of $Ti(BH_4)_3$ such as $Ti(BH_4)_3(PMe_3)_2$.[1,32,33] No Ti^{IV} tetrahydroborates have been isolated; evidently this oxidation state is reduced by BH_4^-.

In contrast to the bidentate BH_4^- bonding geometry observed in $Ti(\eta^2\text{-}BH_4)_2(dmpe)_2$, the reaction of $VCl_2(dmpe)_2$[25] with $NaBH_4$ in tetrahydrofuran gives the *unidentate* vanadium tetrahydroborate complex $V(\eta^1\text{-}BH_4)_2(dmpe)_2$ (**2**).[34] This formally 15-electron species is isolated as dark purple prisms

$$VCl_2(dmpe)_2 + 2NaBH_4 \rightarrow V(\eta^1\text{-}BH_4)_2(dmpe)_2 + 2NaCl$$

after crystallization from toluene. Alternative preparations of $V(BH_4)_2(dmpe)_2$ involve the reaction of $VOCl_3$ with $LiBH_4$ and excess dmpe or the addition of dmpe to $V(BH_4)_3(PMe_3)_2$,[34] although these methods proceed in lower yield. The magnetic moment of 3.6 μ_B for **2** is similar to those of the chloro and methyl analogues[25] and indicates the presence of three unpaired electrons. Apart from strong broad B–H stretching bands of equal intensity at 2312 and 2095 cm^{-1}, the IR spectrum contains an intense absorption at 1057 cm^{-1}; bands in this region have been attributed in other molecules to the characteristic BH_3 deformation mode of unidentate BH_4^- ligands.[12] The deuterium-substituted analogue $V(BD_4)_2(dmpe)_2$ possesses corresponding B–D stretching modes at 1751, 1558, and 813 cm^{-1}. The ν_H/ν_D ratios of 1.30–1.34 are quite comparable to the 1.32–1.35 values found for $Cu(\eta^1\text{-}BH_4)(PMePh_2)_3$.[12] The room-temperature ^1H NMR spectrum again indicates that the molecule has a trans geometry, and as before, the BH_4^- protons could not be located.

The X-band ESR spectrum of **2** in a frozen toluene solution at −196 °C displays two broad features at ca. 150 and 380 mT; no hyperfine structure was evident in either absorption. Analysis of the ESR spectrum may be performed by using the Hamiltonian

$$H = \beta B{\cdot}g{\cdot}S + D[S_z^2 - \tfrac{1}{3}S(S+1) + \lambda(S_x^2 - S_y^2)] + S{\cdot}A{\cdot}I$$

where D is a zero-field splitting parameter and λ is a symmetry parameter that can vary from zero for axial symmetry to one-third for maximum possible rhombic symmetry.[35] In the analysis, g was assumed to be isotropic and equal to 2.00, as usual for octahedral d^3 species.[36,37] The values $D = 0.23$ cm^{-1} and $\lambda = 0.07$ were obtained by matching the observed resonances to calculated transitions using the D-B plot method for $S = {}^3/_2$ spin states.[36,37] The λ parameter indicates that the molecule possesses near-axial symmetry ($\lambda < 0.1$) and is consistent with a trans stereochemistry. The zero-field splitting parameter is considerably smaller than those of 0.46 and 0.85 cm^{-1} for $VCl_2(dmpe)_2$ and $VMe_2(dmpe)_2$[25] and is indicative of increased ionicity (poorer σ and π overlap) in the $V-BH_4$ bond.[38]

The tetrahydroborate complex $V(BH_4)_2(dmpe)_2$ reacts cleanly with 2 equiv of methyl lithium to give the known vanadium(II) alkyl $VMe_2(dmpe)_2$.[25] Compound **2** does not react with excess dmpe or with H_2 (6 atm) and decomposes under CO to give $dmpe{\cdot}BH_3$ as the only isolable product. Treatment of **2** with *n*-butyllithium under H_2 results in reduction to $V(dmpe)_3$.[39] Compound **2** adds to the small number of known tetrahydroborate derivatives of vanadium: representatives have been described in which the vanadium center adopts +1,[40] +2,[41–43] and +3[43–47] oxidation states.

The results obtained in the titanium and vanadium systems prompted a study of the chromium analogue. The chromium(II) chloride complex $CrCl_2(dmpe)_2$[25] reacts with $NaBH_4$ in tetrahydrofuran

$$CrCl_2(dmpe)_2 + 2NaBH_4 \rightarrow Cr(BH_4)H(dmpe)_2 + 2NaCl + \tfrac{1}{2}B_2H_6$$

---

(23) Marks, T. J.; Kolb, J. R. *Chem. Rev.* **1977**, *77*, 263–293.

(24) Mancini, M.; Bougeard, P.; Burns, R. C.; Mlekuz, M.; Sayer, B. G.; Thompson, J. I. A.; McGlinchey, M. J. *Inorg. Chem.* **1984**, *23*, 1072–1078.

(25) Girolami, G. S.; Wilkinson, G.; Thornton-Pett, M.; Hursthouse, M. B. *J. Chem. Soc., Dalton Trans.* **1985**, 1339–1348.

(26) Burg, A. B. *J. Am. Chem. Soc.* **1961**, *83*, 2226–2231.

(27) Nöth, H.; Hartwimmer, R. *Chem. Ber.* **1960**, *93*, 2238–2245.

(28) Melmed, K. M.; Coucouvanis, D.; Lippard, S. J. *Inorg. Chem.* **1973**, *12*, 232–236.

(29) Soloveichik, G. L.; Bulychev, B. M.; Semenenko, K. N. *Sov. J. Coord. Chem. (Engl. Transl.)* **1978**, *4*, 913–919.

(30) Semenenko, K. N.; Lobkovskii, E. B.; Shumakov, A. I. *J. Struct. Chem. (Engl. Transl.)* **1976**, *17*, 912–914.

(31) Hoekstra, H. R.; Katz, J. J. *J. Am. Chem. Soc.* **1949**, *71*, 2488–2492.

(32) Jensen, J. A.; Wilson, S. R.; Girolami, G. S. *J. Am. Chem. Soc.* **1988**, *110*, 4977–4982.

(33) Franz, H.; Fusstetter, H.; Nöth, H. *Z. Anorg. Allg. Chem.* **1976**, *427*, 97–113.

(34) Jensen, J. A.; Girolami, G. S. *J. Am. Chem. Soc.* **1988**, *110*, 4450–4451.

(35) Dowsing, R. D.; Gibson, J. F. *J. Chem. Phys.* **1969**, *50*, 294–303.

(36) Hempel, J. C.; Morgan, L. O.; Lewis, W. B. *Inorg. Chem.* **1970**, *9*, 2064–2072.

(37) Dowsing, R. D.; Gibson, J. F.; Goodgame, M.; Hayward, P. J. *J. Chem. Soc. A* **1969**, 187–193.

(38) Kosky, C. A.; Gayda, J.-P.; Gibson, J. F.; Jones, S. F.; Williams, D. J. *Inorg. Chem.* **1982**, *21*, 3173.

(39) Chatt, J.; Watson, H. R. *J. Chem. Soc.* **1962**, 2545–2549.

(40) Kinney, R. J.; Jones, W. D.; Bergman, R. G. *J. Am. Chem. Soc.* **1978**, *100*, 7902–7915.

(41) Cotton, F. A.; Duraj, S. A.; Roth, W. J. *Inorg. Chem.* **1984**, *23*, 4113–4115.

(42) Cotton, F. A.; Duraj, S. A.; Falvello, L. R.; Roth, W. J. *Inorg. Chem.* **1985**, *24*, 4389–4393.

(43) Jensen, J. A.; Girolami, G. S. *Inorg. Chem.* following paper in this issue.

(44) Marks, T. J.; Kennelly, W. J. *J. Am. Chem. Soc.* **1975**, *97*, 1439–1443.

(45) Hessen, B.; Teuben, J. H.; Lemmen, T. H.; Huffman, J. C.; Caulton, K. G. *Organometallics* **1985**, *4*, 946–948.

(46) Makhaev, V. D.; Semenenko, K. N. *Bull. Acad. Sci. USSR, Div. Chem. Sci. (Engl. Transl.)* **1978**, *27*, 2520–2521.

(47) Makhaev, V. D.; Borisov, A. P.; Mozgina, N. G.; Boiko, G. N.; Semenenko, K. N. *Inorg. Mater. (Engl. Transl.)* **1978**, *14*, 1342–1347.

Table I. Crystallographic Data for $Ti(BH_4)_2(dmpe)_2$ and $V(BH_4)_2(dmpe)_2$

	$TiB_2P_4C_{12}H_{40}$	$VB_2P_4C_{12}H_{40}$
T, °C	25	−75
space group	$P2_1/n$	$P2_1/n$
a, Å	9.404 (2)	8.469 (2)
b, Å	13.088 (2)	13.735 (4)
c, Å	9.466 (2)	9.666 (7)
β, deg	96.12 (1)	96.14 (3)
V, Å^3	1158.4 (4)	1118 (2)
Z	2	2
mol wt	377.87	380.91
ρ_{calcd}, g cm^{-3}	1.083	1.131
λ, Å	0.71073	0.71073
μ_{calcd}, cm^{-1}	6.27	7.01
transmissn coeff	0.804–0.834	0.854–0.899
R_F	0.036	0.032
R_{wF}	0.035	0.030

to yield a red product that may be crystallized as needles from pentane. Microanalytical and infrared data indicate that the product possesses the stoichiometry $Cr(BH_4)H(dmpe)_2$ (**3**). The IR spectrum displays absorptions at 2330, 2071, and 1056 cm^{-1} that are consistent with the presence of a unidentate BH_4^- group[12] and a band at 1580 cm^{-1} that arises from the Cr–H stretching mode of a terminal hydride ligand. The compound is a rare example of a paramagnetic hydride complex: the magnetic moment of $\mu_{eff} = 2.5$ μ_B indicates the presence of two unpaired electrons. This spin state is also adopted by $CrCl_2(dmpe)_2$ and the methyl derivative $CrMe_2(dmpe)_2$.[25]

The ^{1}H NMR spectrum of **3** shows four phosphine resonances (two PCH_2 and two PMe_2 signals) that are consistent with a trans octahedral geometry with inequivalent axial groups. As before, no resonances for the BH_4^- group could be located. In some samples, a second species is present that we believe is *trans*-Cr(η^1-BH_4)$_2$(dmpe)$_2$ (**4**). The bis(tetrahydroborate) complex appears in those ^{1}H NMR samples that contain appreciable amounts of BH_3·dmpe; the borane adduct is often present in solution and is formed upon trace decomposition or hydrolysis of **3**. The ^{1}H NMR spectrum under these conditions contains additional resonances at δ −0.3 (fwhm = 240 Hz) and δ −15.8 (fwhm = 500 Hz) due to the PCH_2 and PMe_2 groups of *trans*-Cr(η^1-BH_4)$_2$(dmpe)$_2$, respectively. The relative amounts of **3** and **4** in solution vary from sample to sample. Deliberate attempts to isolate $Cr(BH_4)_2(dmpe)_2$ by addition of BH_3·THF to $Cr(BH_4)H(dmpe)_2$ have been unsuccessful. $Cr(BH_4)H(dmpe)_2$ does not react with triethylamine and hydrogen but does react with excess dmpe in refluxing tetrahydrofuran to yield $Cr(dmpe)_3$.[39] No other well-established chromium tetrahydroborates are known.[48,49]

The preparation and X-ray crystal structure of $Cr(BH_4)H(dmpe)_2$ have been described previously,[22] but two aspects of this work deserve comment. First, the complex was formulated as having a *bidentate* BH_4^- coordination geometry. While the Cr···B distance of ca. 2.45 Å determined crystallographically[22] is consistent with an η^2-bonding mode, there was evidence of disorder involving the BH_4^- group, and it is possible that the Cr···B distance is underestimated significantly. The IR band at 1056 cm^{-1} observed for $Cr(BH_4)H(dmpe)_2$ is strong evidence in favor of a *unidentate* BH_4^- bonding mode,[12] and we propose that the structure of the complex should be reformulated as Cr(η^1-BH_4)H(dmpe)$_2$. Second, the presence of two species in solution was not recognized. Otherwise, our observations and those previously described[22] are in substantial agreement.

X-ray Crystal Structure of Ti(η^2-BH_4)$_2$(dmpe)$_2$. The molecular structure of Ti(η^2-BH_4)$_2$(dmpe)$_2$ is illustrated in Figure 1, while crystal data, final positional parameters, and selected bond distances and angles are listed in Tables I–III. Hydrogen atoms, including those attached to boron, were readily apparent in the Fourier difference maps and were refined with independent isotropic thermal coefficients. Although the molecule lies on a crystallographic inversion center, the overall symmetry of the complex is very nearly D_{2h}. The titanium center is eight-coordinate but adopts neither the dodecahedral geometry nor the square-antiprismatic geometry usually seen in eight-coordination. Given that the angle subtended at the metal by the tetrahydroborate ligands is fairly small (53°), the structure can best be viewed as a trans octahedron where the bidentate tetrahydroborate ligands are considered to occupy one site each. This latter view is justified by the intramolecular distances: the Ti–H bonds are rather long at 2.06 (2) Å, and the Ti···B contact of 2.534 (3) Å is longer than

Table II. Final Atomic Coordinates for $Ti(BH_4)_2(dmpe)_2$ and $V(BH_4)_2(dmpe)_2$

	x/a	y/b	z/c
	$Ti(BH_4)_2(dmpe)_2$		
Ti	0.0	0.0	0.5
P1	0.19873 (6)	0.11366 (5)	0.40355 (6)
P2	0.14820 (6)	0.06666 (5)	0.73249 (6)
C1	0.0583 (4)	0.1292 (3)	0.8701 (4)
C2	0.2704 (6)	−0.0172 (4)	0.8383 (5)
C3	0.2618 (6)	0.1715 (4)	0.6823 (4)
C4	0.3300 (4)	0.1477 (4)	0.5513 (4)
C5	0.1500 (5)	0.2353 (3)	0.3220 (6)
C6	0.3136 (5)	0.0618 (4)	0.2772 (6)
B	0.1635 (3)	−0.1533 (2)	0.4914 (3)
H1	0.126 (2)	−0.098 (1)	0.401 (2)
H2	0.106 (2)	−0.129 (2)	0.589 (2)
H3	0.286 (3)	−0.150 (2)	0.514 (3)
H4	0.132 (3)	−0.232 (2)	0.464 (3)
H1a	0.120 (3)	0.158 (2)	0.938 (3)
H1b	−0.003 (4)	0.182 (3)	0.829 (4)
H1c	0.005 (4)	0.076 (3)	0.915 (4)
H2a	0.324 (3)	−0.053 (3)	0.780 (4)
H2b	0.330 (4)	0.023 (3)	0.900 (5)
H2c	0.220 (4)	−0.068 (3)	0.889 (4)
H3a	0.322 (3)	0.182 (2)	0.760 (4)
H3b	0.205 (5)	0.223 (4)	0.638 (5)
H4a	0.390 (3)	0.201 (2)	0.521 (3)
H4b	0.390 (4)	0.083 (3)	0.586 (5)
H5a	0.226 (3)	0.270 (3)	0.297 (3)
H5b	0.102 (3)	0.273 (2)	0.377 (3)
H5c	0.082 (4)	0.226 (3)	0.233 (4)
H6a	0.395 (4)	0.107 (2)	0.278 (4)
H6b	0.265 (6)	0.064 (5)	0.192 (6)
H6c	0.345 (5)	0.009 (4)	0.303 (5)
	$V(BH_4)_2(dmpe)_2$		
V	0.0	0.0	0.0
P1	−0.14370 (8)	0.01897 (5)	−0.23809 (7)
P2	0.10071 (8)	−0.14846 (5)	−0.11309 (7)
C1	−0.0561 (3)	−0.0683 (2)	−0.3508 (3)
C2	−0.0239 (3)	−0.1658 (2)	−0.2782 (3)
C3	−0.1443 (5)	0.1316 (3)	−0.3378 (4)
C4	−0.3523 (4)	−0.0152 (3)	−0.2584 (4)
C5	0.2984 (4)	−0.1410 (3)	−0.1672 (5)
C6	0.1001 (5)	−0.2696 (2)	−0.0376 (4)
B	0.2379 (5)	0.1181 (3)	−0.0993 (5)
H1a	−0.122 (3)	−0.075 (2)	−0.437 (3)
H1b	0.036 (3)	−0.043 (2)	−0.372 (2)
H2a	−0.123 (3)	−0.191 (2)	−0.252 (3)
H2b	0.024 (3)	−0.211 (2)	−0.341 (3)
H3a	−0.196 (3)	0.119 (2)	−0.431 (3)
H3b	−0.044 (4)	0.154 (3)	−0.339 (4)
H3c	−0.201 (4)	0.174 (2)	−0.294 (3)
H4a	−0.403 (3)	0.034 (2)	−0.211 (3)
H4b	−0.367 (3)	−0.075 (2)	−0.221 (3)
H4c	−0.395 (4)	−0.012 (2)	−0.354 (4)
H5a	0.374 (3)	−0.141 (2)	−0.087 (3)
H5b	0.307 (4)	−0.088 (2)	−0.216 (3)
H5c	0.323 (4)	−0.195 (3)	−0.220 (4)
H6a	0.121 (3)	−0.317 (2)	−0.103 (3)
H6b	0.012 (4)	−0.280 (2)	−0.009 (4)
H6c	0.185 (4)	−0.272 (2)	0.038 (3)
H1	0.192 (4)	0.058 (2)	−0.037 (3)
H2	0.239 (4)	0.099 (3)	−0.208 (4)
H3	0.360 (4)	0.121 (3)	−0.066 (4)
H4	0.190 (5)	0.180 (3)	−0.084 (5)

---

(48) Nöth, H.; Seitz, M. *J. Chem. Soc., Chem. Commun.* **1976**, 1004.

(49) Koola, J. D.; Brintzinger, H. H. *J. Chem. Soc., Chem. Commun.* **1976**, 388–389.

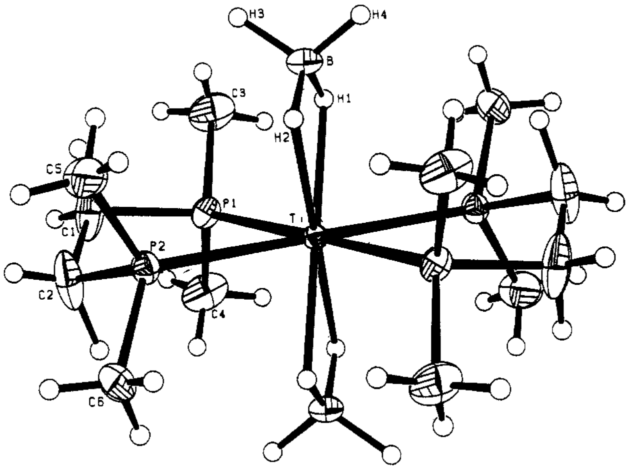

Figure 1. ORTEP diagram of $Ti(\eta^2\text{-}BH_4)_2(dmpe)_2$ (**1**). Thermal ellipsoids are drawn at the 35% probability level, and hydrogen atoms are represented as arbitrarily sized spheres.

Table III. Selected Distances (Å) and Angles (deg) for $Ti(BH_4)_2(dmpe)_2$ and $V(BH_4)_2(dmpe)_2$

$Ti(BH_4)_2(dmpe)_2$		$V(BH_4)_2(dmpe)_2$	
	Bond Distances		
Ti-P1	2.627 (1)	V-P1	2.499 (1)
Ti-P2	2.625 (1)	V-P2	2.506 (1)
Ti···B	2.534 (3)	V···B	2.833 (4)
Ti-H1	2.04 (2)	V-H1	1.88 (3)
Ti-H2	2.09 (2)		
C3-C4	1.488 (6)	C1-C2	1.523 (4)
B-H1	1.14 (2)	B-H1	1.12 (3)
B-H2	1.16 (2)	B-H2	1.09 (4)
B-H3	1.15 (2)	B-H3	1.05 (4)
B-H4	1.09 (3)	B-H4	0.95 (5)
	Bond Angles		
P1-Ti-P2	76.67 (2)	P1-V-P2	80.68 (2)
P1-Ti···B	88.88 (7)	P1-V-H1	97.4 (10)
P2-Ti···B	91.15 (7)	P2-V-H1	85.0 (10)
H1-Ti-H2	53.0 (8)		
Ti-H1-B	102 (1)	V-H1-B	140 (3)
Ti-H2-B	98 (1)		
H1-B-H2	107 (1)	H1-B-H2	112 (3)
H1-B-H3	110 (2)	H1-B-H3	104 (3)
H1-B-H4	111 (2)	H1-B-H4	113 (3)
H2-B-H3	113 (2)	H2-B-H3	101 (3)
H2-B-H4	108 (2)	H2-B-H4	114 (3)
H3-B-H4	108 (2)	H3-B-H4	110 (3)

the 2.46 Å predicted by adding the 1.6-Å ionic radius of a bidentate tetrahydroborate group[50] with the 0.86-Å ionic radius of octahedral titanium(II).[51]

The geometry about boron is almost perfectly tetrahedral: the H-B-H angles all fall in the narrow range 107 (1)-113 (2)°. The unperturbed tetrahedral geometry around boron is unusual for metal tetrahydroborates, where small but statistically and chemically significant deviations away from a regular tetrahedron are usually seen. For example, in $Cp_2Ti(BH_4)$, the H_b-B-H_b angle has closed to 91 (7)°, while the H_t-B-H_t angle has opened to 129 (9)°.[28] Furthermore, the B-H_b distance in $Cp_2Ti(BH_4)$ of 1.40 (10) Å is longer than the B-H_t distance of 1.23 (8) Å. The titanium(III) tetrahydroborate $Ti(BH_4)_3(PMe_3)_2$ contains a bidentate BH_4^- group with similar distortions away from a regular tetrahedron.[32] These values are in marked contrast to those in $Ti(BH_4)_2(dmpe)_2$, where the bridging H1-B-H2 angle is 107 (1)° and the terminal H3-B-H4 angle is 108 (2)°. The B-H distances are also unusually regular at 1.14 (2), 1.16 (2), 1.15 (2), and 1.09 (3) Å, so that there is no difference in B-H_b and B-H_t bond lengths. The overall geometry of the BH_4^- groups in $Ti(BH_4)_2(dmpe)_2$ suggests that the interaction between Ti and BH_4^- is weak and essentially electrostatic. Further evidence in favor of this description may be obtained from the IR spectra (see below).

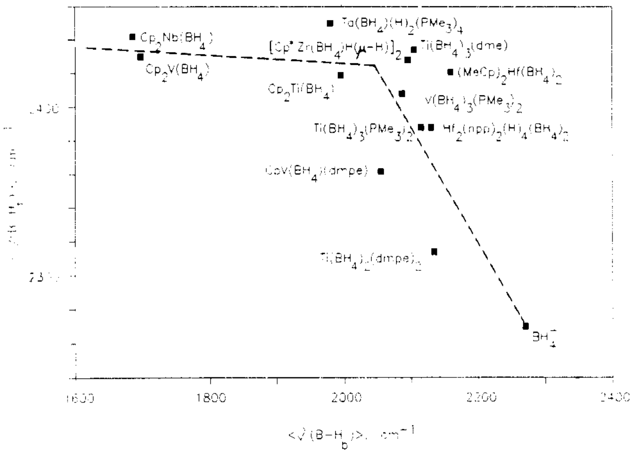

Figure 2. Infrared spectra as a gauge of M-BH_4 bond strength for bidentate tetrahydroborate complexes $Cp_2Nb(BH_4)$,[44,61] $Cp_2V(BH_4)$,[44] $Ta(BH_4)H_2(PMe_3)_4$,[8] $[Cp^*Zr(BH_4)H(\mu\text{-}H)]_2$,[62] $Ti(BH_4)_3(MeOCH_2CH_2OMe)$,[1] $Cp_2Ti(BH_4)$,[27] $(C_5H_4Me)_2Hf(BH_4)_2$,[63] $V(BH_4)_3(PMe_3)_2$,[34] $Ti(BH_4)_3(PMe_3)_2$,[32] $Hf_2(BH_4)_2H_4(npp)_2$,[9] $CpV(BH_4)(dmpe)$,[45] $Ti(BH_4)_2(dmpe)_2$ (this work), and BH_4^-.[64]

The average Ti-P distance of 2.626 (1) Å is slightly longer than those in other divalent titanium species: e.g., 2.586 (5), 2.514 (4), and 2.533 (6) Å in $TiCl_2(dmpe)_2$,[25] $TiMe_2(dmpe)_2$,[10,52] and $(C_5H_4Me)_2Ti(dmpe)$.[53]

It is instructive to compare the structure of high-spin $Ti(\eta^2\text{-}BH_4)_2(dmpe)_2$ with the analogous low-spin complex, $CrH_4(dmpe)_2$.[54] Both compounds are d^2 and eight-coordinate, but unlike the titanium compound, the Cr^{IV} hydride adopts a conventional D_{2d} dodecahedral geometry with the hydrides at the inner (A) sites and the dmpe ligands bridging between the outer (B) sites of the two interpenetrating trapezoids. The M-H and M-P distances in the chromium complex of 1.57 (3) and 2.255 (3) Å are significantly shorter than the 2.06 (2) and 2.626 (1) Å distances in $Ti(BH_4)_2(dmpe)_2$; the smaller atomic radius of chromium and the higher oxidation state of $CrH_4(dmpe)_2$ account for its low-spin, diamagnetic electronic configuration.

Infrared Spectra as a Gauge of M-BH_4 Bond Strength. The X-ray crystallographic studies indicate that the Ti-BH_4 interaction in $Ti(\eta^2\text{-}BH_4)_2(dmpe)_2$ is unusually weak, and this conclusion is supported by comparisons of IR stretching frequencies in **1** with those of other bidentate tetrahydroborate complexes. For $M(\eta^2\text{-}BH_4)$ complexes, the average of the symmetric and antisymmetric terminal B-H stretching frequencies, $\langle\nu(BH_t)\rangle$, and the average bridging B-H stretching frequency, $\langle\nu(BH_b)\rangle$, can be used as a gauge of the strength of the M-BH_4 interaction. Specifically, as the strength of the M-BH_4 interaction increases, the $\langle\nu(BH_b)\rangle$ frequency decreases significantly while the $\langle\nu(BH_t)\rangle$ frequency increases slightly; this is consistent with the expected weakening of the BH_b bonds (and strengthening of the BH_t bonds) as the M-H_b bonds become stronger.[44]

Figure 2 shows these two parameters for a variety of structurally characterized transition-metal complexes with bidentate tetrahydroborate groups. The graph may be divided into three regions. Region I contains complexes such as $Cp_2Nb(BH_4)$ and $Cp_2V(BH_4)$ that display strong covalent bonding between the metal and the tetrahydroborate groups.[44] These species are marked by the presence of very low-energy B-H_b stretching frequencies. Region II encompasses all but one of the remaining complexes and can be described as the "normal" $\nu(BH_t)$ and $\nu(BH_b)$ positions for

---

(50) Edelstein, N. *Inorg. Chem.* **1981**, *20*, 297-299.

(51) Shannon, R. D. *Acta. Crystallogr., Sect A: Cryst. Phys., Diffr., Theor. Gen. Crystallogr.* **1976**, *A32*, 751-767.

(52) Jensen, J. A.; Morris, R. J.; Wilson, S. R.; Schultz, A. J.; Girolami, G. S. Manuscript in preparation.

(53) Girolami, G. S.; Wilkinson, G.; Thornton-Pett, M.; Hursthouse, M. B. *J. Chem. Soc., Dalton Trans.* **1984**, 2347-2350.

(54) Salt, J. E.; Girolami, G. S.; Wilkinson, G.; Motevalli, M.; Thornton-Pett, M.; Hursthouse, M. B. *J. Chem. Soc., Dalton Trans.* **1985**, 685-692.

Table IV. Structural Comparisons of Unidentate Tetrahydroborate Groups and Related Species[a]

compd	M–H_b, Å	B–H_b, Å	B–H_t, Å	M···B, Å	M–H_b–B, deg	M–H_b–B–H_t, deg	ref
$V(\eta^1\text{-}BH_4)_2(dmpe)$ (**2**)	1.88 (3)	1.12 (3)	1.03 (5)	2.833 (4)	140 (3)	–53 (5), 78 (4), –173 (4)	this work
$Fe(\eta^1\text{-}BH_4)H(dmpe)_2$ (**5**)	1.72	1.14	1.10	2.84	161.7	–53, 73, –171	18
$Cu(\eta^1\text{-}BH_4)(PMePh_2)_3$ (**6**)	1.697 (5)	1.170 (5)	1.23 (5)	2.518 (3)	121.7 (4)	–28, 90, –158	14
$Cu(\eta^1\text{-}BH_4)(triphos)$[b] (**7**)	1.60 (4)	1.19[c]	1.19[c]	2.44 (2)	121 (3)	–54, 67, –173	16
$Ti(BH_4)_3(PMe_3)_2$[d]	1.73 (7)	0.95 (6)	0.96 (6)	2.27 (1)	112 (5)	–28 (7), 94 (7), –151 (5)	32
$Hf_2(BH_4)_3H_3(npp)_2$[e]	1.93 (6)	1.29[c]	1.21[c]	2.636 (7)	108	–14, 106, –134	9

[a] Distances in Å and angles in deg. [b] triphos = $MeC(CH_2PPh_2)_3$. [c] BH_4 group refined as rigid body with the B–H distance constrained. [d] "side-on" BH_4 coordination. [e] Intermediate between η^1 and η^2; npp = $N(SiMe_2CH_2PMe_2)_2$.

bidentate early-transition-metal tetrahydroborates. In these species, neither covalent bonding nor ionic bonding predominates. Finally, region III contains the complex $Ti(BH_4)_2(dmpe)_2$, which possesses a very weak Ti–BH_4 interaction. As can be seen from the graph, $Ti(BH_4)_2(dmpe)_2$ lies closer to the free BH_4^- ion than any other tetrahydroborate compound. We suggest that in this compound, *one* metal orbital is interacting with the BH_4 group, A, unlike the bonding in other bidentate tetrahydroborate species, which is usually considered to involve *two* metal orbitals, B.[23,24] Accordingly, the description of the structure of $Ti(BH_4)_2(dmpe)_2$ as a trans octahedron rather than as an eight-coordinate species may be justifiable on electronic as well as geometric grounds. In any case, the Ti–BH_4 bond in **1** is weak and unusually ionic for a transition-metal tetrahydroborate complex.

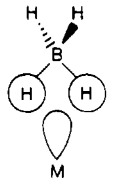

A

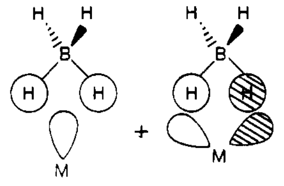

B

X-ray Crystal Structure of $V(\eta^1\text{-}BH_4)_2(dmpe)_2$. Single crystals of **2** were obtained by cooling saturated tetrahydrofuran solutions to –20 °C; crystal data are given in Table I, while final atomic parameters and important bond lengths and angles are given in Tables II and III. Hydrogen atoms were located in the difference maps and refined independently as in the titanium structure above. Although **1** and **2** are crystallographically isomorphous, the vanadium center in **2** is clearly octahedral and the tetrahydroborate ligands are *unidentate* (Figure 3). The P–V–P angle of 80.68 (2)° is larger than that in the titanium complex, and this is solely a consequence of the shorter V–P bonds of 2.503 (1) Å. This distance may be compared with the 2.37–2.57-Å range found in other vanadium(II) phosphine complexes: 2.374 (1) Å in $Cp_2V_2H_2(dmpe)_3$,[55] 2.467 (1) Å in $CpV(BH_4)(dmpe)$,[45] 2.499 (5) Å in $VCl_2(dmpe)_2$,[25] 2.523 (1) Å in $V(oep)(PMePh_2)_2$,[56] 2.525 (2) Å in $V_2(BH_4)_2Cl_2(dmpm)_2$,[41] and 2.569 (4) Å in $V_2(BH_4)_2Cl_2(dppm)_2$.[42]

The tetrahydroborate groups deviate only slightly from an idealized tetrahedral geometry. For example, the B–H_b bonds of 1.12 (3) Å are, as expected, longer than the 1.03 (5) Å B–H_t bonds, although the difference is of only marginal significance statistically. The H–B–H angles of 104 (3)–114 (3)°, however, do not exhibit any chemically significant deviations from an ideal tetrahedron. The V–H distance of 1.88 (3) Å is comparable with those in previously reported vanadium tetrahydroborate complexes, and the long V···B distance of 2.833 (4) Å clearly establishes the η^1-BH_4 geometry. The unidentate BH_4^- bonding mode in **2** vs the bidentate bonding mode in the titanium analogue **1** is probably attributable to the smaller size of vanadium and to the preference of d^3 species to adopt octahedral coordination environments.

Structural Comparisons of Unidentate Tetrahydroborates. Since only three other unidentate tetrahydroborate complexes have been crystallographically characterized, it is of interest to compare the structures of these species with that of $V(BH_4)_2(dmpe)_2$. The metric parameters pertaining to the η^1-BH_4 groups are collected in Table IV; also included in the table are data for two related compounds: $Ti(BH_4)_3(PMe_3)_2$, which contains a "side-on" BH_4^- group,[32] and $Hf_2[N(SiMe_2CH_2PMe_2)_2]_2H_3(BH_4)_3$, which contains a BH_4^- group that is apparently intermediate between an η^1- and an η^2-bonding mode.[17]

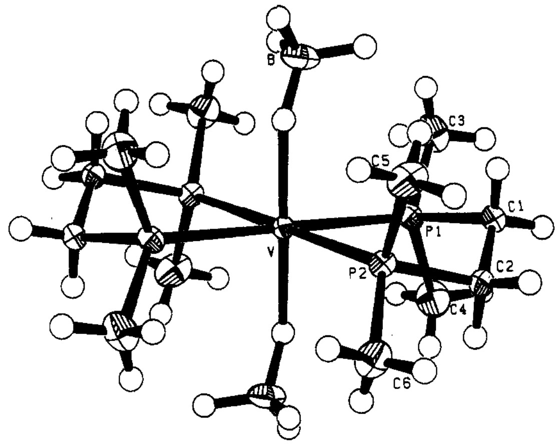

Figure 3. ORTEP diagram of $V(\eta^1\text{-}BH_4)_2(dmpe)_2$ (**2**). Thermal ellipsoids are drawn at the 35% probability level, and hydrogen atoms are represented as arbitrarily-sized spheres.

The M–H_b–B angle of 140 (3)° in **2** is intermediate between the 162° angle in $Fe(\eta^1\text{-}BH_4)H(dmpe)_2$ (**5**) and the 121° angles in the copper complexes $Cu(\eta^1\text{-}BH_4)(PMePh_2)_3$ (**6**) and $Cu(\eta^1\text{-}BH_4)[MeC(CH_2PPh_2)_3]$ (**7**). Overall, the structures of the two dmpe complexes **2** and **5** are rather similar: the B–H_b and M···B distances and the M–H_b–B–H_t torsion angles are virtually identical. Only the M–H_b distances in **2** and **5** differ appreciably, due to the 0.18 Å larger ionic radius of vanadium(II) vs low-spin iron(II).

Edelstein[50] has demonstrated that the M···B distances in bidentate and tridentate BH_4^- complexes can be predicted with fair accuracy by adding an effective BH_4^- ionic radius of 1.6 Å (for η^2 groups) or 1.36 Å (for η^3 groups) to the ionic radius[51] of the complexed metal. A similar attempt to deduce an effective ionic radius for unidentate BH_4^- ligands results in a range of values: 2.04 Å in **2**, 2.23 Å in **5**, 1.92 Å in **6**, and 1.84 Å in **7**. The 0.40-Å spread is a consequence of the flexibility of the M–H_b–B linkage; such flexibility is not possible in bidentate or tridentate geometries. Thus, it is of little use to ascribe a single value for the ionic radius of a unidentate BH_4^- group. However, if subtraction of the metal ionic radius from the M···B distance in a particular compound gives a value of 1.8 Å or greater, it is likely that the BH_4^- ligand is unidentate.

The M–H_b–B–H_t torsion angles in compounds **2**, **5**, **6**, and **7** fall into two classes. The two dmpe compounds **2** and **5** and $Cu(\eta^1\text{-}BH_4)[MeC(CH_2PPh_2)_3]$ (**7**) adopt staggered configurations in which the metal is disposed more-or-less symmetrically with respect to two gauche terminal hydrogen atoms; this is apparent from a Newman diagram projected down the B–H_b bond (Figure 4a). The M–H_b–B–H_t torsion angles of –53, +73, and –172° are within about 10° of the idealized values of –60, +60, and –180° for a perfect staggered arrangement. Presumably, this

---

(55) Hessen, B.; van Bolhuis, F.; Teuben, J. H.; Petersen, J. L. *J. Am. Chem. Soc.* **1988**, *110*, 295–296.

(56) Poncet, J.-L.; Barbe, J.-M.; Guilard, R.; Oumous, H.; Lecomte, C.; Protas, J. *J. Chem. Soc., Chem. Commun.* **1982**, 1421–1422.

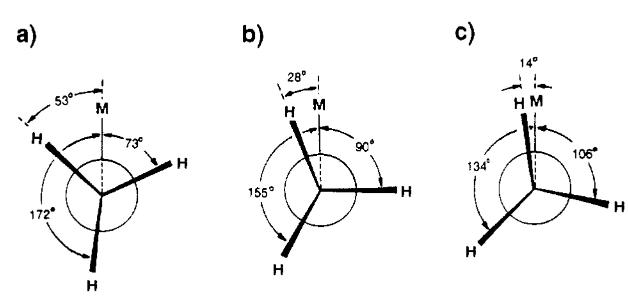

Figure 4. Newman diagrams of η^1-BH_4 complexes projected down the B–H_b bond: (a) for the complexes $V(\eta^1\text{-}BH_4)_2(dmpe)_2$ (**2**), $Fe(\eta^1\text{-}BH_4)H(dmpe)_2$ (**5**), and $Cu(\eta^1\text{-}BH_4)[MeC(CH_2PPh_2)_3]$ (**7**); (b) for $Cu(\eta^1\text{-}BH_4)(PMePh_2)_3$ (**6**) and $Ti(BH_4)_3(PMe_3)_2$; (c) for $Hf_2(BH_4)_3H_3[N(SiMe_2CH_2PMe_2)_2]_2$.

geometry minimizes nonbonded repulsions between the terminal B–H hydrogen atoms and the ligands on the metal center.

Interestingly, the first crystallographically characterized unidentate tetrahydroborate complex, $Cu(\eta^1\text{-}BH_4)(PMePh_2)_3$ (**6**) is the exception: the torsion angles of −28, +90, and −158° are roughly halfway between an eclipsed and a staggered geometry (Figure 4b). This arrangement brings one of the three terminal B–H hydrogen atoms closer to the copper center than the other two. While this Cu···H contact of 2.73 Å is definitely outside of the bonding range, it has been described as an "incipient Cu–H bonding interaction."[14] Compound **6** is known to dissociate in solution to give free $PMePh_2$ and the bidentate BH_4^- complex $Cu(\eta^2\text{-}BH_4)(PMePh_2)_2$,[12] and the incipient bonding interaction results in one hydrogen atom being "poised" for coordination to the Cu center upon dissociation of one of the phosphine ligands.[14] Thus, compound **6** can be thought of as an early intermediate along a reaction coordinate connecting unidentate and bidentate BH_4^- groups.

The "side-on" tetrahydroborate complex $Ti(BH_4)_3(PMe_3)_2$ possesses torsion angles of −28, 94, and −151° that are very similar to those of $Cu(\eta^1\text{-}BH_4)(PMePh_2)_3$. In this case, the geometry is adopted not to bring a terminal hydrogen closer to the metal center but to create a Ti–B bonding interaction.[32]

The last complex in Table IV, $Hf_2(BH_4)_3H_3[N(SiMe_2CH_2PMe_2)_2]_2$, contains one BH_4^- group that exhibits Hf–H_b–B–H_t torsion angles of −14, +106, and −134° (Figure 4c). These values are very near those of 0, +120, and −120° expected for an idealized bidentate BH_4^- ligand, and the authors accurately described this geometry to be intermediate between an η^1- and η^2-bonding mode.[9]

In fact, the series of Newman projections in Figure 4 nicely describes a reaction coordinate connecting η^1- and η^2-bonding modes. This reaction coordinate consists of a rotation about the B–H_b bond from a nearly staggered (Figure 4a) to a nearly eclipsed geometry (Figure 4c). This motion may resemble the mechanism of terminal–bridge hydrogen exchange that is characteristic of bidentate BH_4^- groups. The breaking of one M–H bond of a bidentate BH_4^- ligand and subsequent rotation of the unidentate BH_4^- group has been proposed previously to account for terminal–bridge hydrogen exchange processes,[57–60] but the structural data given here provide the first detailed look at such a reaction coordinate and the probable geometry of its transition state.

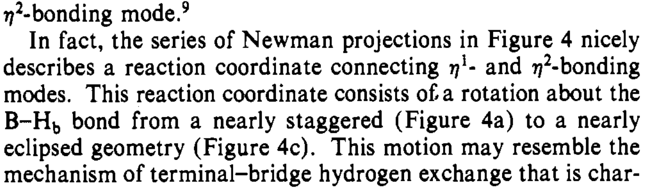

Experimental Section

All operations were carried out in vacuum or under argon by using standard techniques. Solvents were distilled from sodium (toluene) or sodium–benzophenone (pentane, diethyl ether, tetrahydrofuran) under nitrogen immediately before use. The $MCl_2(dmpe)_2$ complexes[25] and $V(BH_4)_3(PMe_3)_2$[34] were prepared as described previously, while $LiBH_4$ (Strem), $NaBH_4$ (Alfa), and $NaBD_4$ (Cambridge Isotopes) were used as received. $VOCl_3$ (Alfa) was distilled before use.

Microanalyses were performed by the University of Illinois Microanalytical Laboratory. The IR spectra were recorded on a Perkin-Elmer 599B instrument as Nujol mulls. The proton NMR data were recorded on a Perkin-Elmer R-24B instrument at 60 MHz, on a Varian EM-390 instrument at 90 MHz, or on a General Electric QE-300 instrument at 300 MHz. Chemical shifts are uncorrected for the paramagnetic shift of the solvent, and are reported in δ units (positive shifts to high frequency) relative to TMS. Magnetic moments were determined in toluene by a modification of Evans' method.[65] Melting points were determined in closed capillaries under argon.

Bis(tetrahydroborato)bis[1,2-bis(dimethylphosphino)ethane]titanium(II). To a slurry of $LiBH_4$ (0.48 g, 22.3 mmol) in diethyl ether (50 mL) at −78 °C was added a solution of $TiCl_2(dmpe)_2$ (1.81 g, 4.32 mmol) in diethyl ether (200 mL) at −78 °C. The solution was stirred for 2 h at −78 °C and then 2 h at room temperature. The solvent was removed under vacuum, and the residue was extracted with toluene (200 mL). The filtered extract was concentrated to ca. 170 mL and cooled to −20 °C. Red-orange prisms of the complex were isolated, and several further crops of crystals were obtained by concentration and cooling of the supernatant. Yield: 1.25 g (77%). Mp: 195 °C dec. Anal. Calcd for $C_{12}H_{40}B_2P_4Ti$: C, 38.1; H, 10.7; B, 5.7; Ti, 12.7. Found: C, 38.2; H, 10.8; B, 5.6; Ti, 12.8. ^1H NMR (C_6D_6, 25 °C): δ 11.39 (s, fwhm = 775 Hz, PCH_2), −2.35 (s, fwhm = 290 Hz, PMe_2). Magnetic moment (toluene, 25 °C): $\mu = 2.6\ \mu_B$. IR (Nujol, cm^{-1}): 2336 s, 2299 s, 2215 s, 2170 s, 2138 m, 2026 w, 1415 s, 1298 m, 1281 m, 1262 w, 1170 w, 1136 w, 1113 s, 1021 w, 993 w, 944 s, 925 s, 890 m, 862 w, 833 w, 794 w, 731 m, 701 m, 643 m, 430 w.

Bis(tetradeuterioborato)bis[1,2-bis(dimethylphosphino)ethane]titanium(II). To $NaBD_4$ (0.36 g, 8.60 mmol) was added a solution of $TiCl_2(dmpe)_2$ (0.57 g, 1.36 mmol) in tetrahydrofuran (70 mL). The solution was stirred at room temperature for 20 h. The solvent was removed under vacuum, and the residue was extracted with toluene (75 mL) and worked up as above. Yield: 0.32 g (61%). IR (Nujol, cm^{-1}): 1765 w, 1750 s, 1705 s, 1662 s, 1623 m, 1582 m, 1525 w, 1415 s, 1295 m, 1280 m, 1262 w, 1175 w, 1130 w, 1080 w, 990 w, 940 s, 920 s, 885 m, 865 w, 835 m, 830 sh, 795 w, 725 s, 695 s, 640 s, 430 w.

Bis(tetrahydroborato)bis[1,2-bis(dimethylphosphino)ethane]vanadium(II). Method A. To $VCl_2(dmpe)_2$ (1.54 g, 3.6 mmol) and $NaBH_4$ (0.71 g, 18.8 mmol) was added tetrahydrofuran (120 mL). After the mixture was stirred for 30 h at 25 °C, the originally deep purple solution had turned pale pink. The solvent was removed under vacuum and the residue extracted with toluene (150 mL). The filtered extract was concentrated to ca. 120 mL and cooled to −20 °C. Dark purple crystals of the complex were isolated, and several further crops of crystals were obtained by concentration and cooling of the supernatant. The crystals turn gray when dried under vacuum. Yield: 1.18 g (86%). Mp: 140 °C dec. Anal. Calcd for $C_{12}H_{40}B_2P_4V$: C, 37.8; H, 10.6; V, 13.4. Found: C, 37.8; H, 10.4; V, 13.5. ^1H NMR (C_6D_6, 25 °C): δ −8.6 (s, fwhm = 500 Hz, PCH_2), −19.3 (s, fwhm = 950 Hz, PMe_2). Magnetic moment (toluene, 25 °C): $\mu = 3.6\ \mu_B$. IR (Nujol, cm^{-1}): 2341 sh, 2312 vs b, 2110 sh, 2095 vs b, 1422 s, 1300 m, 1282 m, 1136 w, 1086 w, 1057 vs, 992 w, 956 vs, 944 vs, 932 s, 889 m, 865 w, 846 w, 833 m, 797 w, 736 m, 706 m, 633 m, 439 w.

Method B. To $VOCl_3$ (1.0 mL, 10.6 mmol) in diethyl ether (50 mL) was added dropwise a solution of $LiBH_4$ (1.65 g, 75.8 mmol) in diethyl ether (150 mL). The initially dark red $VOCl_3$ solution proceeded through aqua, blue, black, and finally violet stages as the tetrahydroborate solu-

---

(57) Williams, R. E. *J. Inorg. Nucl. Chem.* **1961**, *20*, 198–204.
(58) James, B. D.; Nanda, R. K.; Wallbridge, M. G. H. *J. Chem. Soc. A* **1966**, 182–184.
(59) Letts, J. B.; Mazanec, T. J.; Meek, D. W. *J. Am. Chem. Soc.* **1982**, *104*, 3898–3905.
(60) A concerted mechanism involving an η^3-BH_4 transition state has also been proposed: (a) Marks, T. J.; Shimp, L. A. *J. Am. Chem. Soc.* **1972**, *94*, 1542–1550. (b) Barone, V.; Dolcetti, G.; Lelj, F.; Russo, N. *Inorg. Chem.* **1981**, *20*, 1687–1691.
(61) Lucas, C. R.; Green, M. L. H. *J. Chem. Soc., Chem. Commun.* **1972**, 1005.
(62) Wolczanski, P. T.; Bercaw, J. E. *Organometallics* **1982**, *1*, 793–799.
(63) Johnson, P. L.; Cohen, S. A.; Marks, T. J.; Williams, J. M. *J. Am. Chem. Soc.* **1978**, *100*, 2709–2715.
(64) Price, W. C. *J. Chem. Phys.* **1949**, *17*, 1044–1052.
(65) Evans, D. F.; Fazakerley, G. V.; Phillips, R. F. *J. Chem. Soc. A* **1971**, 1931–1934.

tion was added. After the addition was completed, the solution was stirred an additional 2 h and then was filtered into a −78 °C receiving flask. To this solution was added 1,2-bis(dimethylphosphino)ethane (3.5 mL, 21.1 mmol), causing the violet solution to turn dark green. The solution was warmed to 0 °C, and the solution turned gray. The solvent was removed under vacuum, and the residue was extracted with toluene (240 mL). The toluene extract was filtered, concentrated to ca. 190 mL, and cooled to −20 °C. Purple crystals of the complex were isolated, and several further crops of crystals were obtained by concentration and cooling of the supernatant. The crystals turned gray when dried under vacuum. Yield: 1.95 g (49%).

Method C. To $V(BH_4)_3(PMe_3)_2$ (0.25 g, 1.0 mmol) dissolved in diethyl ether (50 mL) at −78 °C was added 1,2-bis(dimethylphosphino)ethane (1.0 mL, 6.0 mmol). The solution was stirred for 15 min at −78 °C and then slowly warmed to room temperature. Upon warming, the green solution turned red. After 2 h at room temperature, a green precipitate formed and the solution color slowly discharged. After 4 h, the solution was colorless and a dark colored precipitate formed. The solvent was removed in vacuum, and the residue was extracted with toluene (20 mL). The toluene extract was filtered, concentrated to ca. 12 mL, and cooled to −20 °C. Purple crystals of the complex were isolated, and several subsequent crops were obtained by concentration and cooling of the supernatant. Yield: 0.17 g (45%).

Bis(tetradeuterioborato)bis[1,2-bis(dimethylphosphino)ethane]vanadium(II). The deuterio analogue $V(BD_4)_2(dmpe)_2$ was obtained from $VCl_2(dmpe)_2$ (0.27 g, 0.6 mmol) and $NaBD_4$ (0.13 g, 3.1 mmol) in tetrahydrofuran (50 mL) in a manner analogous to the preparation of $V(BH_4)_2(dmpe)_2$. Purple crystals were isolated from toluene. Yield: 0.15 g (64%). IR: (Nujol, cm^{-1}): 1751 s, 1696 w, 1558 s, 1423 s, 1299 m, 1282 m, 1138 w, 1088 w, 994 w, 955 s, 946 s, 933 m, 890 m, 867 w, 836 m, 813 m, 737 m, 707 m, 646 m, 440 w.

Hydrido(tetrahydroborato)bis[1,2-bis(dimethylphosphino)ethane]chromium(II). To a mixture of $CrCl_2(dmpe)_2$ (0.95 g, 2.2 mmol) and $NaBH_4$ (0.34 g, 9.0 mmol) was added tetrahydrofuran (80 mL). The mixture was stirred at room temperature for 8 h, and the solution color slowly changed from green to red. The solvent was removed under vacuum, and the residue was extracted with pentane (200 mL). The filtered extract was concentrated to ca. 150 mL and cooled to −20 °C. Bright red needles of the complex were isolated, and several further crops of crystals were obtained by concentration and cooling of the supernatant. Yield: 0.40 g (48%). Mp: 120 °C dec. Anal. Calcd for $C_{12}H_{37}BP_4Cr$: C, 37.7; H, 10.6; B, 2.9; Cr, 13.6. Found: C, 37.7; H, 10.5; B, 2.7; Cr, 13.5. ^1H NMR (C_6D_6, 25 °C) δ −13.3 (s, fwhm = 300 Hz, P*Me*$_2$), −25.8 (s, fwhm = 150 Hz, P*CH*$_2$), −30.1 (s, fwhm = 200 Hz, P*CH*$_2$), −34.2 (s, fwhm = 210 Hz, P*Me*$_2$). Magnetic moment (toluene, 25 °C): 2.5 μ_B. IR (Nujol, cm^{-1}): 2370 sh, 2330 m, 2070 m, 1587 m, 1550 sh, 1421 m, 1291 m, 1277 m, 1258 w, 1226 w, 1116 w, 1069 m, 986 w, 937 s, 927 s, 887 m, 861 w, 830 w, 785 m, 724 m, 694 m, 634 m, 601 w, 500 w, 454 w, 362 m.

Crystallographic Studies.[66] Single crystals of the divalent titanium tetrahydroborate complex $Ti(\eta^2\text{-}BH_4)_2(dmpe)_2$, grown from toluene, were sealed in thin-walled glass capillaries under argon. [The vanadium complex $V(\eta^1\text{-}BH_4)_2(dmpe)_2$ was crystallized from tetrahydrofuran and mounted similarly; subsequent comments in brackets will refer to this compound.] Preliminary photographs yielded rough cell dimensions, and a suitable crystal was transferred to the diffractometer. Standard peak search and automatic indexing procedures, followed by least-squares refinement using 25 reflections yielded the cell dimensions given in Table I.

Data were collected in one quadrant of reciprocal space ($\pm h,+k,+l$) [$(\pm h,-k,-l)$]. Systematic absences for $0k0$, $k \neq 2n$, and $h0l$, $h + l \neq 2n$, were consistent only with space group $P2_1/n$. The measured intensities were reduced to structure factor amplitudes and their esd's and corrected for background, scan speed, Lorentz and polarization effects, and crystal decay (<6%). [No crystal decay correction was necessary for the vanadium complex.] Absorption corrections were applied. Six reflections flooded the counter and were deleted; only those data with $I > 2.58\sigma(I)$ were used in the least-squares refinement.

The structure was solved by direct methods (MULTAN) [SHELXS-86]; correct positions for the titanium [vanadium] and phosphorus atoms were deduced from an E map. The quantity minimized by the least-squares program was $\sum w(|F_o| - |F_c|)^2$, where $w = 2.75/(\sigma(F_o)^2 + (pF_o)^2)$ [$w = 1.12/(\sigma(F_o)^2 + (pF_o)^2)$]. Analytical approximations to the scattering factors were used, and all scattering factors were corrected for both the real and imaginary components of anomalous dispersion. Weighted difference Fourier syntheses gave positions for the remaining non-hydrogen atoms, and subsequent least-squares difference Fourier calculations revealed positions for all of the hydrogen atoms. In the final cycle of least-squares refinement, all atomic positions were independently refined, non-hydrogen atoms with independent anisotropic thermal coefficients and hydrogen atoms with isotropic thermal coefficients. Successful convergence was indicated by the maximum shift/error of 0.072 [0.001] for the last cycle. Final agreement parameters are given in Table I. The final difference Fourier map had no significant features, and there were no apparent systematic errors among the final observed and calculated structure factors. [The final difference Fourier map for the vanadium compound revealed a minor rotational disorder in the positions of atoms H2, H3, and H4 about the B–H1 bond vector. Refinement of a disordered model converged with an asymmetric site occupancy factor of 0.62 (4) but did not significantly improve the weighted residual; the disordered model was accordingly rejected. A final analysis of variance between observed and calculated structure factors showed a very slight dependence on sin θ.]

Acknowledgment. We thank the National Science Foundation (Grant CHE 85-21757) and the Office of Naval Research under their Young Investigator Award Program for support of this research. We particularly wish to thank Dr. Scott Wilson, Charlotte Stern, and Connie Odle of the University of Illinois X-ray Crystallographic Laboratory for performing the crystal structure determinations. G.S.G. is the recipient of an A. P. Sloan Foundation Research Fellowship (1988–1990) and a Henry and Camille Dreyfus Teacher-Scholar Award (1988–1993).

Registry No. **1**, 111662-13-6; **2**, 114692-86-3; **3**, 107934-18-9; **4**, 120172-64-7; $Ti(BD_4)_2(dmpe)_2$, 120172-61-4; $V(BD_4)_2(dmpe)_2$, 120172-62-5; $TiCl_2(dmpe)_2$, 94631-21-7; $VCl_2(dmpe)_2$, 100760-11-0; $V(BH_4)_3(PMe_3)_2$, 114692-85-2; $CrCl_2(dmpe)_2$, 86747-55-9; dmpe·BH_3, 120172-63-6; $VMe_2(dmpe)_2$, 100647-40-3; $V(dmpe)_3$, 75878-45-4; $Cr(dmpe)_3$, 75862-30-5.

Supplementary Material Available: Tables S1–S5, giving full crystallographic details, anisotropic thermal parameters, and complete bond distances and angles for **1** and **2** (5 pages); tables of final observed and calculated structure factors for **1** and **2** (16 pages). Ordering information is given on any current masthead page.

---

(66) For a full description of the crystallographic procedure, see ref 32.